Preprints of the 21st IFAC World Congress (Virtual)
Berlin, Germany, July 12-17, 2020

Facade-Integrated Semi-Active Vibration Control for Wind-Excited Super-Slender Tall Buildings

Yangwen Zhang * **Thomas Schauer** ** **Laurenz Wernicke** **
Wulf Wulff * **Achim Bleicher** *

* *Chair of Hybrid Structures - Structural Concrete, Brandenburg University of Technology, 03046 Cottbus, Germany, (e-mail: yangwen.zhang@b-tu.de).*
** *Control Systems Group, Technische Universität Berlin, 10587 Berlin, Germany*

Abstract: Nowadays, skyscrapers are getting higher and more slender due to inner-city concentration, which makes the structure more susceptible to dynamic excitations. The design of super-slender skyscrapers is governed primarily by wind excitation. A traditional Tuned Mass Damper (TMD) has been installed in many skyscrapers to mitigate wind-induced vibrations, which has been proven to be very reliable. However, it needs large additional mass and huge installation space near the top of the building, which makes TMD not optimal for super-slender skyscrapers. In this paper, a semi-active distributed-Multiple Tuned Facade Damper (d-MTFD) using movable facade elements as damping mass is investigated. The facade elements at the upper stories of the building are parallel movable to the primary structure. Electrical Machines (EM) as variable damper are integrated in their connections to realize semi-active vibration control, which makes the system more effective and robust. For real application, a practical design criterion is that the relative displacement of the facade elements cannot be too large, otherwise it makes the occupants feel uncomfortable. Therefore, multi-objective Genetic Algorithm (GA)-optimized on-off groundhook semi-active control is applied, where two control objectives are optimized. One control objective is to minimize the peak top floor acceleration and the other control objective is to minimize the maximum peak relative displacement of all the facade elements. As a result, a Pareto Front shows that better vibration suppression performance and smaller facade relative displacement can be achieved using the multi-objective optimized controller.

Keywords: distributed-Multiple Tuned Facade Damper(d-MTFD), multi-objective optimization, Genetic Algorithm(GA), groundhook semi-active control

1. INTRODUCTION

Due to significant economic benefits in dense urban land use, more and more super-slender tall buildings are built worldwide (Hayes, 2018). Slender skyscrapers are very susceptible to wind excitation. Tuned Mass Damper (TMD) and distributed-Multiple Tuned Mass Damper (d-MTMD) have been widely investigated passively and actively and proven to be very effective solutions to mitigate the structure vibration. However, they both need additional mass and space.

An approach using movable building cladding to isolate the dynamic wind loads from the structural system is first proposed by Kareem (1994), which is similar to the concept of base isolation for buildings under seismic excitation. This approach is further developed by Moon (2009) using Double Skin Facade (DSF). The DSF outer skin can move back and forth perpendicular to the primary structure, to isolate the primary structure from the dynamic wind forces. The primary structure motion can be substantially reduced by using lower stiffness DSF connections and no additional mass is needed. However, the excessive motion of the DSF outer skin is a serious design limitation. To mitigate the facade vibration, Moon (2016) further proposed the TMD and DSF damping (DSFD) interaction system, which requires relatively small additional mass and the facade vibration becomes smaller. Zhang et al. (2019) have also studied the energy harvesting potential of this approach. In Moon's approach, the wind loads act on the movable facade and are transmitted to the primary structure through springs and dampers. However, if the facades are perpendicular movable connected and the system is under seismic excitation, the seismic loads act directly on the primary structure and are transmitted to the movable facades. This system becomes d-MTMD with the facade mass as damping mass. For d-MTMD under seismic excitation, the tuning of the connection is different from facade isolation. Many studies have been conducted to investigate and optimize the vibration control performance of d-MTMD using perpendicular movable facade mass (Abtahi et al., 2012), (Fu, 2013), (Barone et al., 2015), (Fu and Zhang, 2016), (Pipitone et al., 2018).

In this paper, an innovative parallel movable connection solution between the DSF outer skin and primary structure is proposed, so that the facade is fixed in the direction perpendicular to the primary structure, but movable in the direction parallel to the primary structure. The difference between the parallel movable facade and the perpendicular movable facade is illustrated in Fig. 1. For slender skyscrapers under wind excitation, the most governing design criterion is to reduce the wind-induced oscillation in the across-wind direction due to vortex shedding. Using perpendicular movable connection, the movable DSF outer skin on two sides begins to oscillate, then the oscillation transmits to the primary structure. To make the transmission as small as possible is the design objective. However, using parallel movable connection, the wind-induced structure vibration causes the movable DSF outer skin on two sides to vibrate together, which in turn damp out the structure motion. Different from d-MTMD, facade mass is used as damping mass, so no additional mass is needed. Therefore, this system with parallel movable facade connection is named as distributed-Multiple Tuned Facade Damper (d-MTFD).

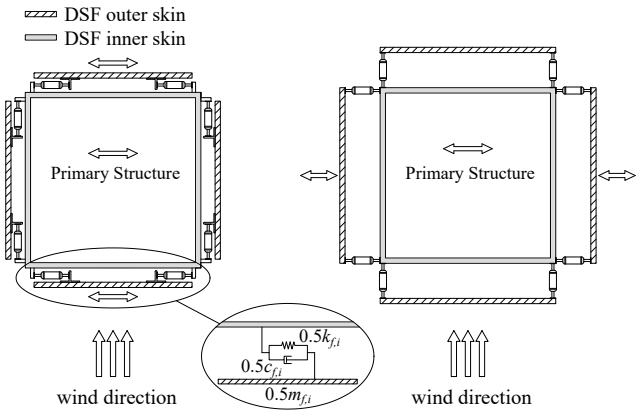

Fig. 1. Concept of the parallel movable DSF outer skin (left) and perpendicular movable DSF outer skin (right).

As shown in the Fig. 1, each side of the two parallel movable DSF outer skin at different stories weighs $0.5m_{f,i}$, and the connection is modeled as the facade connection stiffness $0.5k_{f,i}$ and facade connection damping coefficient $0.5c_{f,i}$. i is introduced to distinguish movable facade at different stories. Therefore, the facade weight at different stories is $m_{f,i}$,where $i = 1, 2, \cdots, n_f$, and the connection is modeled as $k_{f,i}$, $c_{f,i}$. The upper n_f stories are installed with the parallel movable facade. Fig. 2 shows the model of a n story high building installed with parallel movable facade in its upper n_f stories. $m_1, m_2, \cdots, m_n$ are the weights of the building stories and $f_{w,1}, f_{w,2}, \cdots, f_{w,n}$ are the across-wind loads acting on the corresponding stories.

Technically, the d-MTFD system is the same as the d-MTMD system. However, the facade masses are used as damping mass, so there are more design limitations compared with d-MTMD. The relative displacement of facade elements, i.e. facade displacement relative to its connected story of the building, need to be restricted in a certain range. Therefore, multi-objective Genetic Algorithm (GA) is used to optimize the passive d-MTFD to reduce the peak top floor acceleration and reduce the maximum peak

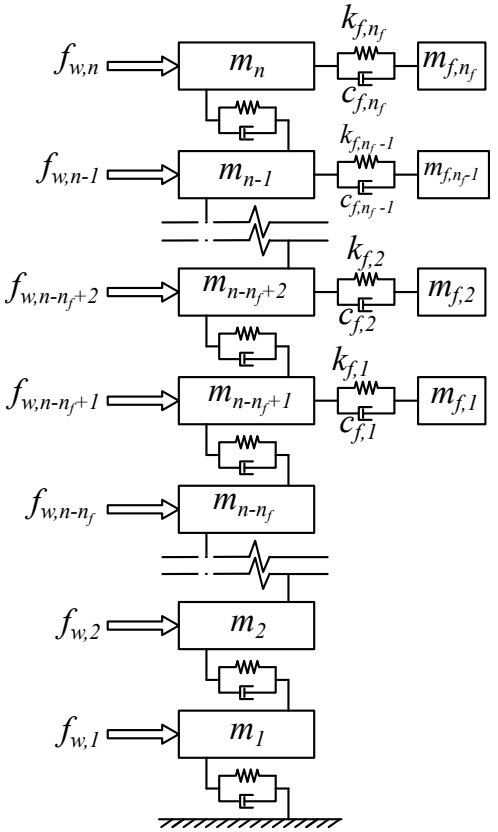

Fig. 2. d-MTFD system modeling.

relative displacement of all the facades. Based on the optimized passive system, groundhook semi-active control is further implemented in the system. The groundhook semi-active control is also optimized using multi-objective GA. Displacement-Based Groundhook (DBG) control and Velocity-Based Groundhook (VBG) control are both investigated and compared. Electrical Machines (EM) are integrated in the facade connections as facade dampers, whose damping coefficient can be set or controlled.

2. SYSTEM MODELING

The governing equations of a tall building installed with d-MTFD can be described as follows:

$$\boldsymbol{M}_s\ddot{\boldsymbol{x}} + \boldsymbol{C}_s\dot{\boldsymbol{x}} + \boldsymbol{K}_s\boldsymbol{x} = \boldsymbol{\eta}\boldsymbol{f}_w, \tag{1}$$

in which $\boldsymbol{M}_s \in \mathbb{R}^{n_s \times n_s}$, $\boldsymbol{C}_s \in \mathbb{R}^{n_s \times n_s}$, $\boldsymbol{K}_s \in \mathbb{R}^{n_s \times n_s}$ are mass, damping, and stiffness matrices of the whole system, where $n_s = n + n_f$. $\boldsymbol{x} = [x_1, x_2, \cdots, x_n, x_{f,1}, x_{f,2}, \cdots, x_{f,n_f}]^T \in \mathbb{R}^{n_s}$, $\dot{\boldsymbol{x}} \in \mathbb{R}^{n_s}$, and $\ddot{\boldsymbol{x}} \in \mathbb{R}^{n_s}$ are the absolute structure and facade displacement, velocity and acceleration vectors, respectively. For passive d-MTFD, $\boldsymbol{C}_s$ is time-invariant and for semi-active d-MTFD, $\boldsymbol{C}_s$ is time-variant. $\boldsymbol{f}_w = [f_{w,1}, f_{w,2}, \cdots, f_{w,n}]^T \in \mathbb{R}^n$ is the across wind excitation vector and $\boldsymbol{\eta} \in \mathbb{R}^{n_s \times n}$ is the excitation influence matrix.

Solving the above equations with large matrices is very time-consuming. Therefore, modal reduction method is adopted to derive a reduced order model without much loss in the results' accuracy (Preumont, 2018). Ni et al. (2011) have conducted the modal analysis based on a benchmark building and found that the first mode contributes to

93.67% of the total structure acceleration. Under across wind excitation, the high-rise building oscillates near its first natural frequency because of vortex shedding. Hence, all the facade connections can be tuned to the first resonance frequency of the building. Then the whole system can be reduced to a $n_{red} = n_f + 5$ degrees of freedom system, which includes all the facade modes and the first five modes of the building, which has been proven to be accurate enough. The reduced model can be described in the following equation:

$$\boldsymbol{M}_M\ddot{\boldsymbol{z}} + \boldsymbol{C}_M\dot{\boldsymbol{z}} + \boldsymbol{K}_M\boldsymbol{z} = \boldsymbol{\Phi}^T\boldsymbol{\eta}\boldsymbol{f}_w, \tag{2}$$

where $\boldsymbol{M}_M = \boldsymbol{\Phi}^T\boldsymbol{M}_s\boldsymbol{\Phi} \in \mathbb{R}^{n_{red}\times n_{red}}$, $\boldsymbol{C}_M = \boldsymbol{\Phi}^T\boldsymbol{C}_s\boldsymbol{\Phi} \in \mathbb{R}^{n_{red}\times n_{red}}$, $\boldsymbol{K}_M = \boldsymbol{\Phi}^T\boldsymbol{K}_s\boldsymbol{\Phi} \in \mathbb{R}^{n_{red}\times n_{red}}$ are the reduced modal mass, damping, and stiffness matrices. $\boldsymbol{\Phi} \in \mathbb{R}^{n_s\times n_{red}}$ is the matrix of the reduced n_{red} mode shapes. $\boldsymbol{z} = [z_1, z_2, \cdots, z_{n_{red}}]^T \in \mathbb{R}^{n_{red}}$, $\dot{\boldsymbol{z}} \in \mathbb{R}^{n_{red}}$, and $\ddot{\boldsymbol{z}} \in \mathbb{R}^{n_{red}}$ represents the system modal displacement, velocity and acceleration vector, respectively. The relationship between $\boldsymbol{x}$ in nodal coordinates and $\boldsymbol{z}$ in modal coordinates is given by $\boldsymbol{x} = \boldsymbol{\Phi}\boldsymbol{z}$. The governing equation (2) can be easily rewritten in state space form:

$$\begin{aligned}\dot{\boldsymbol{Z}} &= \boldsymbol{A}\boldsymbol{Z} + \boldsymbol{B}\boldsymbol{f}_w\\ \boldsymbol{y_1} &= \boldsymbol{C}_1\boldsymbol{Z} + \boldsymbol{D}\boldsymbol{f}_w\\ \boldsymbol{y_2} &= \boldsymbol{C}_2\boldsymbol{Z}\end{aligned} \tag{3}$$

where the state variables $\boldsymbol{Z} = [\boldsymbol{z}^T, \dot{\boldsymbol{z}}^T]^T \in \mathbb{R}^{2n_{red}}$ are the modal displacement and velocity of the whole system. The performance outputs $\boldsymbol{y_1} = [\ddot{x}_n, x_{f,1} - x_{n-n_f+1}, x_{f,2} - x_{n-n_f+2}, \cdots, x_{f,n_f} - x_n]^T = [\ddot{x}_n, x_{fr,1}, x_{fr,2}, \cdots, x_{fr,n_f}]^T$ are the top floor structural acceleration and relative displacement of facade mass at each story. The measurement outputs $\boldsymbol{y_2} = [x_{n-n_f+1}, x_{n-n_f+2}, \cdots, x_n, \dot{x}_{n-n_f+1}, \dot{x}_{n-n_f+2}, \cdots, \dot{x}_n, \dot{x}_{fr,1}, \dot{x}_{fr,2}, \cdots, \dot{x}_{fr,n_f}]^T$ are the structure displacement and velocity and the facade relative velocity at the upper n_f floors, which are used for the following groundhook semi-active control.

3. MULTI-OBJECTIVE GA OPTIMIZED PASSIVE D-MTFD

The passive d-MTFD system is first optimized using multi-objective GA. The GA is based on the biological principle of optimization through natural selection, which relies on genetic operations, such as mutation, crossover, replication and elitism. In GA, a population consisting of many system solutions with different parameter values compete to find the global minimum of the given cost functions (two selected objectives), and the successful parameter values are propagated to the future generations through a set of genetic rules (Brunton and Kutz, 2019). There is a trade-off between the two selected objectives. Therefore, for multi-objective GA, a Pareto Front will be drawn to plot all the non-inferior cost function values (Deb, 2001). Multi-objective optimization using GA is implemented in the optimization toolbox in MATLAB.

The two objectives selected for the optimization are the minimization of the peak top floor acceleration (i.e. $\min(||\ddot{x}_n||_\infty)$) and the minimization of the peak relative displacement of movable facades at top n_f floors (i.e. $\min(||[x_{fr,1}, x_{fr,2}, \cdots, x_{fr,n_f}]^T||_\infty)$). The top floor acceleration is the most important design criterion for the serviceability of tall buildings under wind excitation (Sarkisian, 2016). Although there are still no codes about the maximum facade movement considering the comfort of the occupants, it is desired to keep the facade motion small.

To use multi-objective GA for the passive d-MTFD system, the optimization parameters need to be selected. To increase the optimization speed, reducing the number of parameters and defining reasonable parameter intervals are necessary. As described in Section 2, the entire facade connection is tuned to the first natural frequency of the structure. Therefore, all the facade connection stiffness coefficients can be calculated as follows:

$$k_{f,i} = m_{f,i}\cdot\omega_1^2 \quad i = (1, 2, \cdots, n_f) \tag{4}$$

where ω_1 is the building's first natural angular frequency and the movable DSF outer skin mass $m_{f,i}$ at story i can be estimated based on its area $A_{f,i}$ (both sides) and area density ρ_A.

For the damping coefficient, the optimum damping ratio of a single TMD system under harmonic excitation can be used as a reference (Den Hartog, 1985), which can be calculated as follows:

$$\begin{aligned}\xi_{ref} &= \sqrt{\frac{3\bar{m}}{8(1+\bar{m})^3}}\\ \bar{m} &= \frac{\sum_{i=1}^{n_f} m_{f,i}}{M_{\text{eff}}}\end{aligned} \tag{5}$$

in which M_{eff} is the first effective modal mass of the structure, whose equation can be found in the reference (Richardson and Jamestown, 2000). As known, the best location for single TMD is where the maximum displacement or acceleration occurs. For d-MTFD, the facade masses are located vertically along the height at the upper floors and the building oscillation primarily follows the first mode. Therefore, with the same damping ratio at each floor, the maximum relative displacement of the facade increases as the floor increases, i.e. $||x_{fr,1}||_\infty < ||x_{fr,2}||_\infty < \cdots < ||x_{fr,n_f}||_\infty$. To make all the facade relative displacement peaks approximately the same, i.e. $||x_{fr,1}||_\infty \cong ||x_{fr,2}||_\infty \cong \cdots \cong ||x_{fr,n_f}||_\infty$, the upper floor damping ratios need to be increased and lower floor damping ratios need to be decreased. Hence, the damping ratio $\xi_{fr,1}$ at lowest floor and the damping ratio ξ_{fr,n_f} at highest floor can be selected as optimizing parameters in GA and the remaining facade damping ratios are assumed to be linearly interpolated. The interval for $\xi_{fr,1}$ and ξ_{fr,n_f} can be reasonably determined based on ξ_{ref}. Then the corresponding facade damping coefficients can be calculated as:

$$c_{f,i} = 2\xi_{fr,i}\sqrt{m_{f,i}k_{f,i}} \quad i = (1, 2, \cdots, n_f) \tag{6}$$

Through this simplification, only two parameters that are restricted in the interval must be optimized, which greatly improves the speed of optimization.

4. MULTI-OBJECTIVE GA OPTIMIZED SEMI-ACTIVE GROUNDHOOK CONTROL

Based on the optimized passive d-MTFD, groundhook semi-active control is implemented in the system by using EM as variable damper. Multi-objective GA is further used to optimize the controller.

In the early 1970s, the famous skyhook control has been developed to reduce the response of vehicles (Karnopp et al., 1974). Skyhook control is designed to reduce the vibration of the sprung mass, i.e. the damping mass, so it is not suitable for control of civil engineering structures. The groundhook control is altered from the original skyhook control and aims to reduce the vibration of the unsprung mass, i.e. the building structure. The application of groundhook control has also been extended to a building with the single TMD system (Koo et al., 2004). In this paper, Velocity Based Groundhook (VBG) control and Displacement Based Groundhook (DBG) control are examined and compared with each other. In the groundhook control logic, the damper condition is examined to determine whether a high or low state of damping is required, as illustrated in table 1.

Table 1. On-off VBG control logic.

Sign conventions	Damper conditions	Damping state
$\dot{x}_{n-n_f+i} > 0, \dot{x}_{fr,i} > 0$	Extension	off state (low)
$\dot{x}_{n-n_f+i} > 0, \dot{x}_{fr,i} < 0$	Compression	on state (high)
$\dot{x}_{n-n_f+i} < 0, \dot{x}_{fr,i} > 0$	Extension	on state (high)
$\dot{x}_{n-n_f+i} < 0, \dot{x}_{fr,i} < 0$	Compression	off state (low)

$\dot{x}_{n-n_f+i}$ represents the building velocity at story $n-n_f+i$. $\dot{x}_{fr,i}$ represents the DSF outer skin relative velocity at the story $n-n_f+i$ $(i=1,2,\cdots,n_f)$.

These four conditions can be summarized in the following equations:

$$\begin{aligned} &\text{if } \dot{x}_{n-n_f+i}\cdot\dot{x}_{fr,i} \geq 0, \text{ then } c_{f,i} = c_{\text{low},i} \\ &\text{if } \dot{x}_{n-n_f+i}\cdot\dot{x}_{fr,i} < 0, \text{ then } c_{f,i} = c_{\text{high},i} \end{aligned} \tag{7}$$

The on-off DBG control logic is evolved from the on-off VGB control logic by changing the building velocity $\dot{x}_{n-n_f+i}$ to the building displacement x_{n-n_f+i}. Therefore, the on-off DBG control can be summarized as:

$$\begin{aligned} &\text{if } x_{n-n_f+i}\cdot\dot{x}_{fr,i} \geq 0, \text{ then } c_{f,i} = c_{\text{low},i} \\ &\text{if } x_{n-n_f+i}\cdot\dot{x}_{fr,i} < 0, \text{ then } c_{f,i} = c_{\text{high},i} \end{aligned} \tag{8}$$

GA is applied to choose the optimal $c_{\text{low},i}$ and $c_{\text{high},i}$. In Section 3, the passive d-MTFD has been optimized, so the optimized passive facade damping coefficients $c_{f,\text{passive},i}$ can be further used to determine the $c_{\text{low},i}$ and $c_{\text{high},i}$. The low/high damping coefficients of the movable facade connections are defined as follows:

$$\begin{aligned} c_{\text{high},i} &= c_{f,\text{passive},i}\cdot(1+p_1) \\ c_{\text{low},i} &= c_{f,\text{passive},i}\cdot(1-p_2) \end{aligned} \tag{9}$$

The parameters need to be optimized are reduced to p_1 and p_2, which significantly reduces the time for the optimization. p_1 and p_2 are the increasing and decreasing percentages compared with $c_{f,\text{passive},i}$.

The overview of the multi-objective GA optimized on-off DBG/VBG semi-active control is presented in Fig. 3. The semi-active force $\boldsymbol{u} = [u_1, u_2, \cdots, u_{n_f}]^T \in \mathbb{R}^{n_f}$ can be directly calculated by (10) and then act on the whole system.

$$u_i = c_{f,i}\cdot\dot{x}_{fr,i} \quad (i=1,2,\cdots,n_f) \tag{10}$$

Alternatively, the time-varying $c_{f,i}$ can be integrated in the system damping matrix $\boldsymbol{C}_s$. Therefore, for semi-active control, $\boldsymbol{C}_s$ in (1) is time-variant.

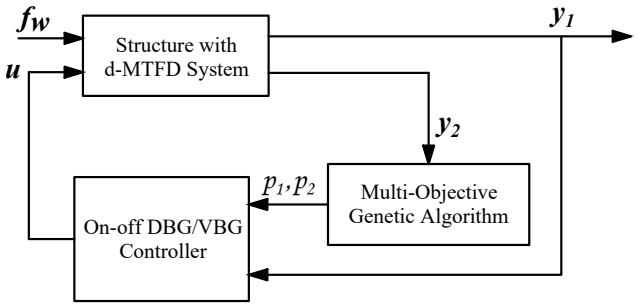

Fig. 3. Overview of the multi-objective GA optimized on-off DBG/VBG semi-active control.

5. RESULTS ANALYSIS

In this paper, a 76-story 306 m benchmark building with an aspect ratio of 7.3 is considered for analysis. Due to its slenderness, it is very wind sensitive. Yang et al. (2004) described all the details and the mathematical model of this benchmark building. In this model, the rotational degrees of freedom have been removed by static condensation and the remaining 76 translational degrees of freedom represent the displacement of floors in the lateral direction. The first five natural frequencies of the building are $0.16, 0.765, 1.992, 3.790$ and 6.395 Hz. 1% damping ratio for the first five modes are assumed using Rayleigh's approach. The across-wind loads acting on the benchmark building are determined from wind tunnel test using a 76-story scaled building model (Samali et al., 2004).

Based on the benchmark model, the upper 30 stories are installed with the parallel movable DSF. The weight of parallel movable DSF outer skin on both sides of each floor can be calculated as: $m_{f,i} = A_{f,i}\rho_A$. The DSF outer skin area on both sides can be estimated to be $320\,\text{m}^2$ at each story, and the area density is estimated as $0.0781\,\text{t/m}^2$. Hence, $m_f = m_{f,1} = m_{f,2} = \cdots = m_{f,30} \approx 25\,\text{t}$ is approximately determined. Because all these 30 connections are tuned to the structure's first natural frequency, all the 30 stiffness coefficients can be calculated using (4). The facade damping ratio at the lowest story and top story are selected as optimizing parameters for GA. According to the calculated reference damping ratio $\xi_{ref} = 0.05$ (the first effective modal mass $M_{\text{eff}} = 111715\,\text{t}$), the lower boundary and upper boundary for both parameters are respectively set to 0.03 and 0.2. The population size is set to 200 and then evolved for 30 generations. The optimized results are presented in the form of Pareto Front, as shown in Fig. 5.

Currently, there are no codes for the allowable relative displacement of movable facades, so $||[x_{fr,1}, x_{fr,2}, \cdots, x_{fr,30}]^T||_\infty \leq 0.5\,\text{m}$ is chosen for the further investigations. When $||[x_{fr,1}, x_{fr,2}, \cdots, x_{fr,30}]^T||_\infty = 0.498\,\text{m}$, the peak top floor acceleration $||\ddot{x}_n||_\infty$ is reduced to $0.183\,\text{m/s}^2$. In this chosen case (Case 1, as marked in Fig. 5), the optimized damping ratios are $\xi_{fr,1} = 0.0575$ and $\xi_{fr,30} = 0.1482$. The remaining damping ratios from $\xi_{fr,2}$ to $\xi_{fr,29}$ are linearly interpolated. With linearly interpolated damping ratios along the height, the difference between each floor's peak facade relative displacement is very subtle and can be neglected, which also proves that the assumption using linear interpolation is reasonable, as shown in Fig. 4.

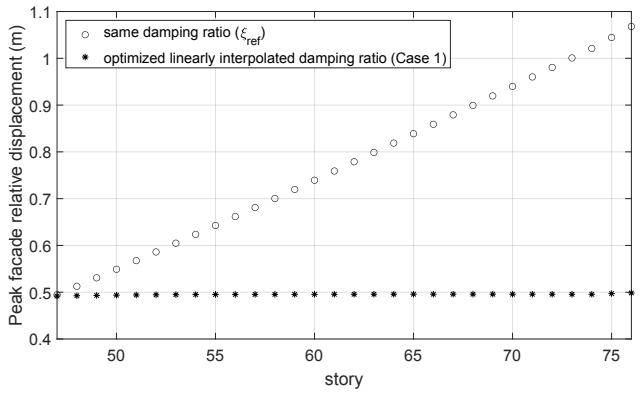

Fig. 4. Peak facade relative displacement at different stories.

Based on (6), the passive facade damping coefficients at each story can be calculated, which will be further used in (9) to determine the optimal low/high damping coefficients for the groundhook semi-active control. The range for the parameter p_1 is limited between 0 to 50%, which is assumed to allow maximum 50% increment for the high damping coefficient, and the range for the parameter p_2 is limited between 0 to 100%, which is assumed that the minimum low damping coefficient can be reduced to 0. The population size is set to 150 and then evolved for 30 generations. The Pareto Front using DBG and VBG control are plotted in Fig. 5 for comparison. By using groundhook semi-active control, both defined objectives can be better optimized compared with the passive d-MTFD system. However, it can be observed that no matter passive or semi-active, the trade-off phenomenon always exists. Under the same boundary conditions, the DBG control is better than the VBG control.

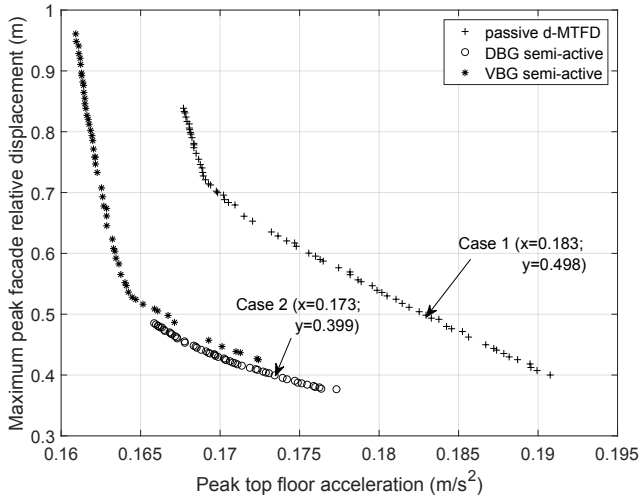

Fig. 5. Pareto Front of multi-objective GA optimized passive and semi-active d-MTFD system.

The Case 2 ($p_1 = 0.3801$, $p_2 = 0.4172$), as marked in Fig. 5, is chosen from the optimized results using DBG semi-active control to compare with Case 1 and uncontrolled structure with fixed facade. The time courses of the top floor displacement x_{76}, top floor acceleration $\ddot{x}_{76}$ and top floor facade relative displacement $x_{fr,30}$ are plotted in Fig. 6 for a wind excitation caused by the reference mean wind speed of 13.5 m/s at 10 m above ground level with a return period of 10 years. The peak top floor displacement $||x_{76}||_\infty$, Root Mean Square (RMS) value of top floor displacement x_{76}^{rms} and the peak top floor acceleration $||\ddot{x}_{76}||_\infty$, RMS value of top floor acceleration $\ddot{x}_{76}^{rms}$ and the peak top floor facade relative displacement $||x_{fr,30}||_\infty$, RMS value of top floor facade relative displacement $x_{fr,30}^{rms}$ are listed in table 2.

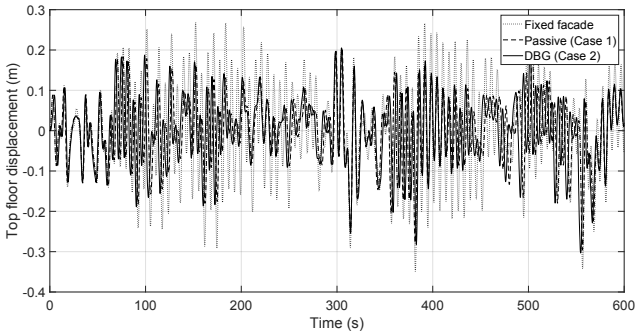

(a) Top floor displacement x_{76}

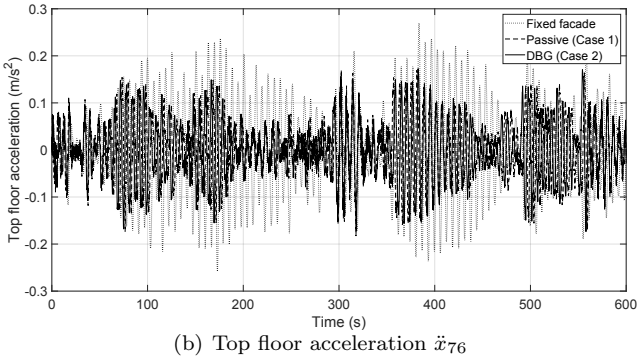

(b) Top floor acceleration $\ddot{x}_{76}$

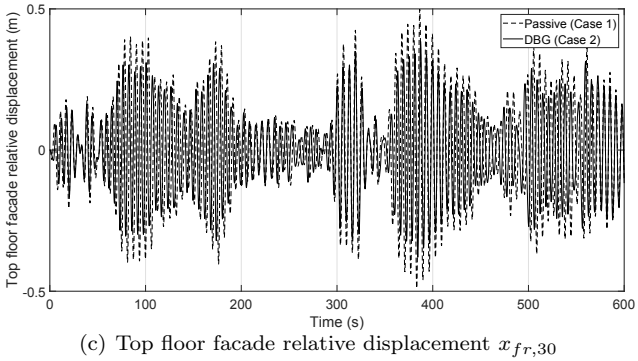

(c) Top floor facade relative displacement $x_{fr,30}$

Fig. 6. Time courses of x_{76}, $\ddot{x}_{76}$ and $x_{fr,30}$ for the structure with fixed facade, Case 1 (Passive) and Case 2 (DBG).

Table 2. Comparison of structure with Fixed facade, Passive (Case 1) and DBG (Case 2).

System	Fixed facade	Passive (Case 1)	DBG (Case 2)
$\|\|x_{76}\|\|_\infty$(m)	0.349	0.296(-15.3%)	0.303(2.6%)
x_{76}^{rms}(m)	0.116	0.081(-30.5%)	0.083(2.4%)
$\|\|\ddot{x}_{76}\|\|_\infty$(m/s^2)	0.270	0.183(-32.2%)	0.174(-5.2%)
$\ddot{x}_{76}^{rms}$(m/s^2)	0.104	0.060(-41.8%)	0.062(2.0%)
$\|\|x_{fr,30}\|\|_\infty$(m)	/	0.498	0.384(-22.9%)
$x_{fr,30}^{rms}$(m)	/	0.178	0.144(-19.1%)

As shown in Fig. 6, the optimized passive and semi-active d-MTFD system both achieve better vibration suppression performance compared with the uncontrolled structure

with fixed facade. For top floor displacement, they all meet the design requirement $h/500$ ($h = 306\,\mathrm{m}$ is the building height), which is relatively easy to satisfy. Therefore, the top floor displacement is not used as a optimization objective. Comparing Case 1 with Case 2, it can be observed that even though the peak top floor acceleration decreases about 5.2% using DBG semi-active control, the RMS value increases only by 2.0%, which is almost unchanged. However, the facade relative displacement can be significantly reduced. The peak top floor facade relative displacement decreases 22.9% and its RMS value decreases 19.1%. Smaller facade vibration is always better for the serviceability of the building. Because of the trade-off phenomenon, the maximum building acceleration can be further reduced with the sacrifice of the vibration of facade. Nevertheless, the reduction of building acceleration is relatively subtle. Therefore, it is more meaningful to use semi-active control to reduce the facade motion.

6. DISCUSSION AND CONCLUSION

In this paper, the innovative d-MTFD is studied using optimized passive control and on-off groundhook semi-active control. Multi-objective GAs are used to find the optimum parameters to reduce the building acceleration, which is an important design criterion for the occupants' comfort, and to reduce the maximum relative displacement of all the parallel movable facades. With this optimization approach, the passive d-MTFD has already shown good performance and the maximum relative displacement of all the facades are kept approximately the same, which takes full advantage of the damping potential of the facade at the lower stories. DBG control and VBG control are both tested and DBG control shows slightly better performance under the same boundary conditions. Using groundhook semi-active control, the facade vibration can be effectively mitigated, which is meaningful for the practical use. The building motion can also be reduced further, but with the sacrifice of more sever facade motion, which is not desired. The realization of the variable damping by EM will be investigated in the next step. A self-contained generator operation is foreseen.

ACKNOWLEDGEMENTS

This publication was funded by the Graduate Research School (GRS) of the Brandenburg University of Technology Cottbus-Senftenberg with the support of the Federal State Government of Brandenburg based on the Postgraduate Scholarship Regulations (GradV) and the research initiative "Future Building" of the Federal Ministry of the Interior, Building and Community, Germany (BMI), (project number: 10.08.18.7-18.22).

REFERENCES

Abtahi, P., Samali, B., Zobec, M., and Ngo, T. (2012). Application of flexible façade systems in reducing the lateral displacement of concrete frames subjected to seismic loads. *From Materials to Structures: Advancement through Innovation*, 241.

Barone, G., Palmeri, A., and Khetawat, A. (2015). Passive control of building structures using double-skin facades as vibration absorbers. in: Kruis, J., Tsompanakis, Y. and Topping, BHV. In *Proceedings of the Fifteenth International Conference on Civil, Structural and Environmental Engineering Computing, Prague, 1st-4th Sept., Paper*, volume 94. c Civil-Comp Press.

Brunton, S.L. and Kutz, J.N. (2019). *Data-driven science and engineering: Machine learning, dynamical systems, and control*. Cambridge University Press.

Deb, K. (2001). *Multi-objective optimization using evolutionary algorithms*, volume 16. John Wiley & Sons.

Den Hartog, J.P. (1985). *Mechanical vibrations*. Courier Corporation.

Fu, T.S. (2013). Double skin facades as mass dampers. In *2013 American Control Conference*, 4742–4746. IEEE.

Fu, T.S. and Zhang, R. (2016). Integrating double-skin facades and mass dampers for structural safety and energy efficiency. *Journal of Architectural Engineering*, 22(4), 04016014.

Hayes, J. (2018). Tall storeys. *Engineering & Technology*, 13(10), 70–73.

Kareem, A. (1994). Methods to control wind-induced building motions. In *Structures Congress XII*, 654–659. ASCE.

Karnopp, D., Crosby, M.J., and Harwood, R. (1974). Vibration control using semi-active force generators.

Koo, J.H., Ahmadian, M., Setareh, M., and Murray, T. (2004). In search of suitable control methods for semi-active tuned vibration absorbers. *Modal Analysis*, 10(2), 163–174.

Moon, K.S. (2009). Tall building motion control using double skin façades. *Journal of architectural engineering*, 15(3), 84–90.

Moon, K.S. (2016). Integrated damping systems for tall buildings: tuned mass damper/double skin facade damping interaction system. *The Structural Design of Tall and Special Buildings*, 25(5), 232–244.

Ni, T., Zuo, L., and Kareem, A. (2011). Assessment of energy potential and vibration mitigation of regenerative tuned mass dampers on wind excited tall buildings. In *ASME 2011 International Design Engineering Technical Conferences and Computers and Information in Engineering Conference*, 333–342. Citeseer.

Pipitone, G., Barone, G., and Palmeri, A. (2018). Optimal design of double-skin façades as vibration absorbers. *Structural Control and Health Monitoring*, 25(2), e2086.

Preumont, A. (2018). *Vibration control of active structures: an introduction*, volume 246. Springer.

Richardson, M.H. and Jamestown, C. (2000). Modal mass, stiffness and damping. *Vibrant Technology, Inc., Jamestown, CA*, 1–5.

Samali, B., Kwok, K., Wood, G., and Yang, J. (2004). Wind tunnel tests for wind-excited benchmark building. *Journal of Engineering Mechanics*, 130(4), 447–450.

Sarkisian, M. (2016). *Designing tall buildings: structure as architecture*. Routledge.

Yang, J.N., Agrawal, A.K., Samali, B., and Wu, J.C. (2004). Benchmark problem for response control of wind-excited tall buildings. *Journal of Engineering Mechanics*, 130(4), 437–446.

Zhang, Y., Schauer, T., and Bleicher, A. (2019). Assessment of wind-induced vibration suppression and energy harvesting using facades. In *20th CONGRESS OF IABSE New York City 2019 - The Evolving Metropolis*, 352–356.